

# Optimizing the impact strength and hardness of the liquid crystal display printed parts using artificial neural network

Mustafa Mohammed Abdulrazaq<sup>1\*</sup>, Vian N. Najm<sup>2</sup>,  
Athraa Mohammed S. Ahmed<sup>3</sup>

<sup>1</sup> Production Engineering and Metallurgy Department, University of Technology-Iraq, Alsina'a street, 10066, Baghdad, Iraq

\* Corresponding author's e-mail: [mustafa.m.abdulrazaq@uotechnology.edu.iq](mailto:mustafa.m.abdulrazaq@uotechnology.edu.iq)

## ABSTRACT

Vat photopolymerization (VPP) is an effective additive manufacturing (AM) process known for its high dimensional accuracy and excellent surface finish. The combination of visible light with the use of LCD screens for 3D printing, allows for a faster, more efficient and economical manufacturing process. Despite these benefits, fabricating the end-use products still has some limitations related to the strength of the fabricated parts. For this purpose, the present paper provides a methodology to predict and optimize three critical process variables in AM, namely: layer height, build orientation, post-curing time. A neural-network model was developed for predicting the impact strength and hardness and optimizing the printing variables for highest responses. From the experiments using full-factorial design, it was revealed that improved parts strength and hardness are obtained at lower layer height, flat orientation, and moderate post-curing time. Based on the ANOVA analysis of, the most effective variable on the impact strength was post-curing time with (41.8%), while the orientation was higher contribution than the rest on the parts hardness with (47.5%). Comparisons between the experimental and the predicted values were illustrated. The mean error between experimental and neural network model was (1.13%) for impact strength and (0.82%) for hardness strength with correlation coefficient equal to 0.988 and 0.982 for the two responses respectively. The current proposed study demonstrates good agreement between the predicted model values and the experiments outcomes of impact strength and parts hardness.

**Keywords:** vat photopolymerization, LCD printing, impact strength, hardness, artificial neural network.

## INTRODUCTION

The concepts of additive manufacturing (AM), also referred to as 3D printing, are becoming increasingly significant among researchers and industry partners [1, 2]. Throughout all photocuring 3D printing technologies, from the laser-scanning of stereolithography (SLA), to digital projection of digital light processing (DLP), to the latest liquid crystal display (LCD) printing technology, the main difference is the light source and imaging system [3], while, the control and stepping system have little difference as shown in Figure 1. The DLP and LCD technologies differ most in their imaging systems [4, 5]. The basis of LCD 3D printing is the employing

of LCD screens as imaging system. The main feature of LCD technique is the way the light beams straight onto the uncured resin from the flat LCD panel [6, 7]. This enables light not to increase, so pixel distortion is less of a problem with LCD process as it occurs with DLP process. Furthermore, unlike in SLA, an entire layer can be exposed simultaneously and there is no necessity for scanning the photopolymer point by point. This benefited from a faster 3D printing speed [8]. Unfortunately, the mechanical issues of printed parts a considered one of the remarkable challenges for the LCD technique specifically for the impact strength and hardness.

Numerous variables have a significant effect on the fabricated part quality, selecting the proper

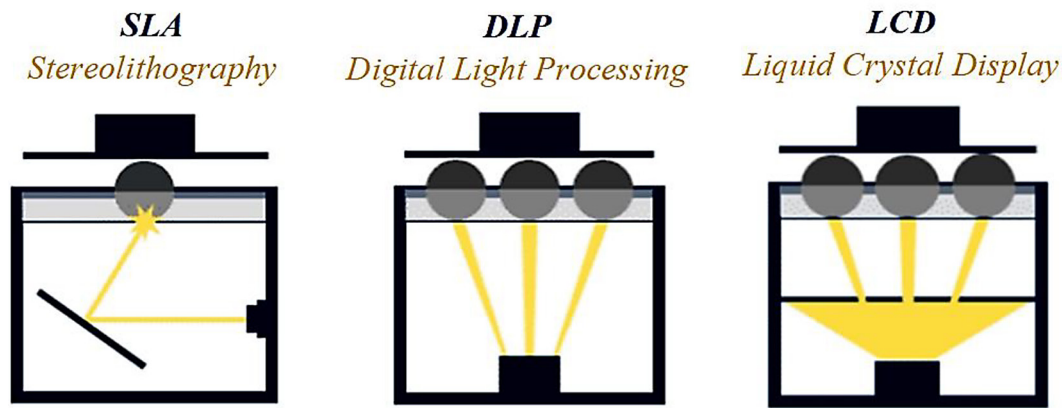


Figure 1. Schematic diagram of the different types of resin printing: SLA, DLP, LCD [9]

parameters combination play an important role in producing the desired properties of the built parts. Selecting the appropriate materials also has a great impact in meeting the required functionality [10, 11]. Some efforts have indicated according to the relevant publications that the mechanical strength is crucial aspect to the quality of the printed components. Riyaz et al. [12] focused on producing 3D printed PLA parts with improved strength and surface quality using LCD 3D printing. Tensile, impact, and flexural specimens with varying layer thicknesses were printed and post-cured to explore the mechanical properties. It was found that by increasing the layer thickness and minimizing the post-curing time, printed samples with maximum strength can be obtained. Al-Dulaijan et al. [13] evaluated the effect of printing orientation combined with different post-curing times on the flexural strength of 3D-printed resins. Their result showed that the highest flexural strength values of 3D-printed resin (NextDent, and ASIGA) were in 0-degree groups. Also, the flexural strength values increased when post-curing time was increased, regardless of the printing orientation.

Seprianto et al. [14] determined the effect of the thickness of the layer and exposure time on the strength, impact toughness applied to the prototype of the reduction gear post, test specimens made using SLA DLP 3D printing. Their results of the analysis revealed that the main factor that had the most influence on the impact strength of the test specimens was the layer Thickness factor with a percentage contribution of 52%, while the interaction between layer thickness and exposure time contributed 6%. Yang et al. [15] investigated the effect of the exposure time of acrylate resin in DLP on the printability and the hardness.

Concerning the mechanical properties, a strong increase in hardness was observed, which went from 0 to 107.2 N as the exposure was varied from 2 to 8 s. Schittecatte et al. [16] reviewed the effect of printing variables, like exposure time and light power on the printed LCD parts hardness. Their study indicates that low exposure times leads to incomplete polymerization, that decreases the specimens' hardness. Al-Wswasi et al. [17] built a neural-network model to predict the compressive strength by varying layer heights, filling pattern and densities. Their model confirmed high accuracy based on result of the regression coefficient.

Based on the previous efforts that investigated the effect of the LCD parameters on the printed part strength and hardness. There are limited investigations that analyzed the impact strength and hardness of printed parts using photopolymerization processes, and these studies did not specifically utilize Art Engineering Resin or LCD printing technology. The presented study tries to tackle this matter. In this regard the article utilizes neural-network model for optimizing the impact strength and hardness of the LCD printed parts based on three critical process parameters: layer height, build orientation, and post-curing time using Art Engineering Resin material.

## MATERIALS AND METHODS

In LCD process, as in many AM technologies, the printed parts characteristics are significantly influenced by a set of factors. To clarify the impact of the printing layer height, build orientation and the post-curing time on the impact strength and hardness of the printed parts in LCD process, 3 levels were assigned for the studied variables in this

work. The regarded printing parameters and the assigned value for each variable are shown in Table 1. A full-factorial experimental design was adopted for conducting tests to obtain the responses' values. A total of 27 combinations were assigned utilizing Minitab program for carrying out the experimental runs and obtaining the impact strength and hardness measures for each corresponding test.

### Specimens preparation and testing

The impact test specimen illustrated in Figure 2a has been designed based on the (ASTM D256) standard, using SolidWorks program. Following the CAD models, the designed files were saved in STL format to enable the slicers to read and slice the models. Chitubox slicer program was utilized as the software to slice the model into subsequent layers, creates support structure, specify print variables and locates the parts within printing platform virtually. Exporting the sliced models as G-code files is essential to make files readable by the printing machine and building the required parts. Figure 2b illustrates the three build positions of the specimens in the slicer.

The samples have been fabricated on “Any-cubic photon mono 6k” printing machine using Art-engineering resin material. After printing the specimens undergo UV light within various periods of time for post-curing process using GCB-1 UV Resin Curing Light Box based on the proposed

design of experiments. To ensure that the result subsequently consistent, a portion of the experiments were replicated. Particularly, about ten of the twenty-seven experiments sets have been replicated within the same combinations. Those experiments were picked to reflect ranges of setting variables and to ensure measurement consistency. While complete replications didn't occur for every set of parameters, the replicated experiments assisted in evaluating experimenting variations and improve the validity of major results. The test specimens for impact strength and hardness test are illustrated Figure 3a, and the utilized LCD printing machine shown in Figure 3b.

For testing the impact strength, the test specimen in this work was a notched rectangular block. Izod impact testing machine was used for performing the impact tests. Figure 4 depicts the experimental setup utilized for conducting the impact tests. The specimen remains a vertical cantilever beam and is broken by a single swing of the pendulum. The pendulum came into initial contact with the specimen on the same side of the notch as shown in Figure 4a. The energy used to break the specimen and depth under the notch in the specimen was used to calculate the impact strength.

Testing the hardness of the printed parts have been performed using Shore D hardness test. After the post-curing process, the specimens were placed on a flat and stable surface. The test was achieved through pressing the digital Shore

**Table 1.** Process variables and levels

No.	Parameter	Symbol	Level			Unit
			(1)	(2)	(3)	
1	Layer height	$h$	0.05	0.075	0.1	mm
2	Build orientation	$O$	Flat (0°)	Upright (90°)	Angled (45°)	degree
3	Post-curing time	$t_c$	2	4	6	min

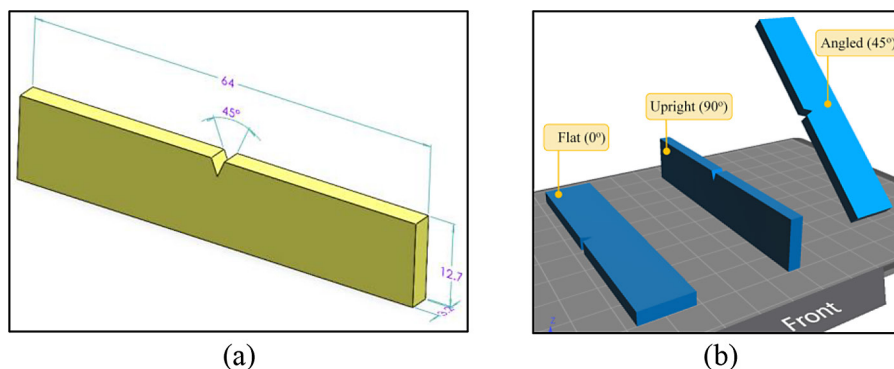


**Figure 2.** Design of specimens, (a) impact test specimen, (b) the build positions in slicing

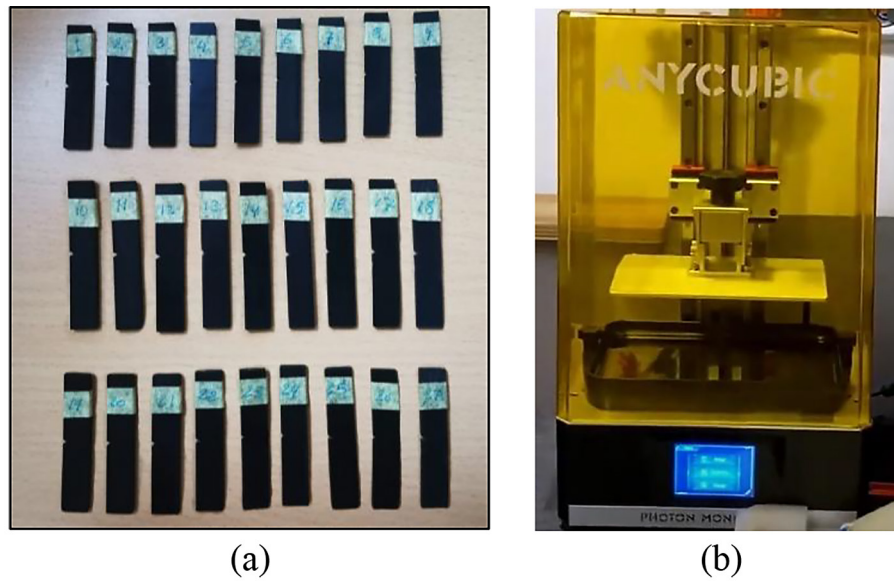


Figure 3. Printed samples by LCD process: (a) impact test specimens, (b) printing machine

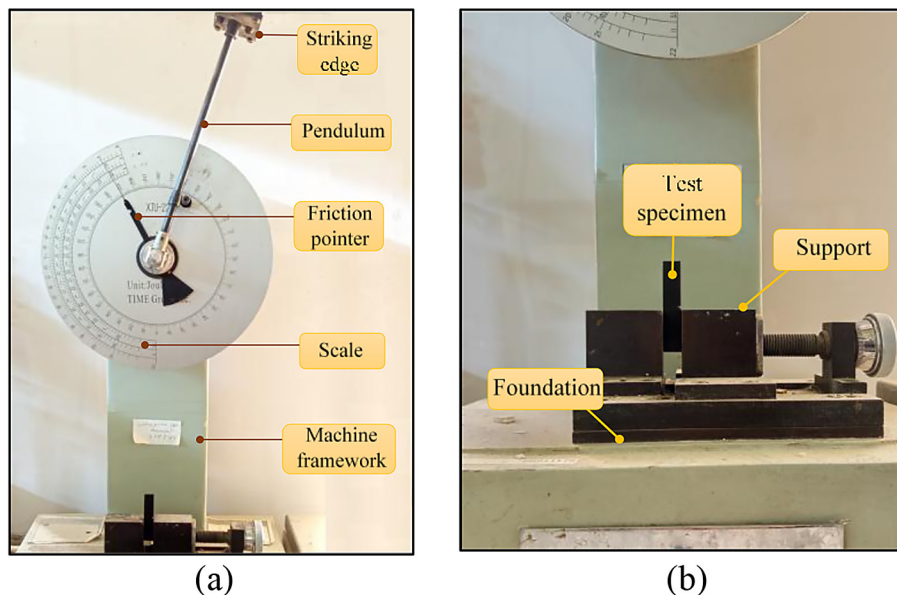


Figure 4. Izod impact testing: (a) Izod tester, (b) specimen held in the vise before striking

Durometer against the samples surfaces with a consistent pressure for (1–3) seconds for each value. The average of five readings for each specimen was taken. Figure 5 shows the Shore Durometer and the test process.

#### Artificial neural network model

The feedforward network has layers are arranged sequentially and it consist of several layers of neurons [18]. The output of one layer serves as input to the neurons of the subsequent layer. Their activation function and neuron count define these

layers [19]. Training the network is a procedure to modify the network weights to obtain the smallest possible deviation between the target of the experimental data and the network output. Backpropagation is the most often applied method for weight adjustment in neural network training [20, 21].

Based on the given values of the impact strength and Shore D hardness from the experiments that carried out using full-factorial experimental design, training the neural network models have been performed between the inputs and outputs. The inputs consist of 3 neurons: layer height ( $h$ ), build orientation ( $O$ ), and post-curing time ( $t_c$ )

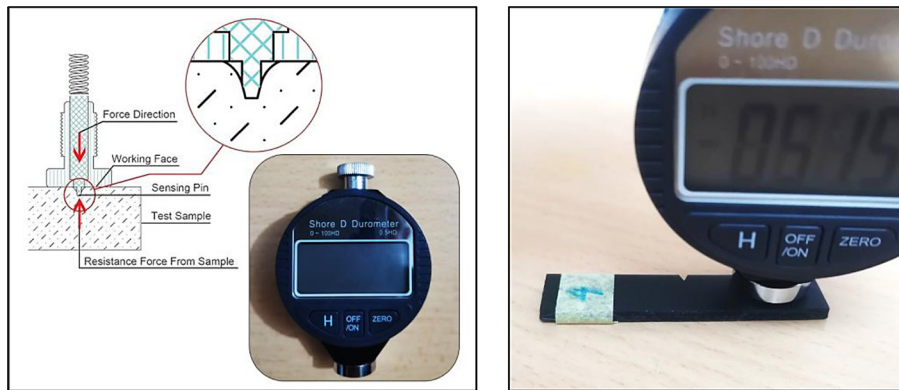


Figure 5. Shore D hardness test for samples: (a) shore durometer, (b) testing of samples

added in  $27 \times 3$  data matrix as illustrated in Figure 6. And 2 neurons have been imported to outputs: impact strength ( $I_s$ ), and hardness ( $HD$ ) in  $27 \times 2$  data matrix. The tangent sigmoid activation function has been used for each layer and feedforward backpropagation network has been created. 70% sample has been used for training, 15% sample for testing and 15% sample for cross-validation. These networks are trained using a back propagation technique that uses the Levenberg Marquardt method. For training moderate sized neural networks using feedforward learning up to several hundred weights, Marquardt algorithm appeared to be the most rapidly approach [22].

## RESULT AND DISCUSSION

### Effect of LCD parameters on impact strength and hardness

The purpose of performing the experiments was mainly for estimating the impact strength and Shore D hardness. The outcomes of the experimental tests are illustrated in Table 2 that is adopted by full factorial design. Based on the results of measuring the printed parts strength, it can be noted that higher impact strength  $9.49 \text{ KJ/m}^2$  and hardness  $77.92 \text{ HD}$  are obtained at lower layer height, moderate post-curing time and flat

position of build orientation. The impact of the individual variables clarified in Figure 7 for each of impact strength and hardness. The illustrated plots show the behavior of the individual parameters on the process outputs, which is known as main effect plots.

The lower layers thickness increased the contact regions among the adjacent layers, which enhanced the adhesion between them and improved the durability and strength of the fabricated parts, giving higher impact strength. Reducing the heights of layers minimizing the gap and voids in the interlayer structures that decreased the porosity, consequently increased the build parts hardness. Using moderate post curing time 4 min provides adequate polymer cross linking avoiding the excessive curing for the printed samples contributing to higher impact strength. That level of post curing produces stable material characteristics through eliminating the inner stresses and enhance the integrity of the build structure of the fabricated parts, and that stability providing optimum polymer cross linking and it is important to achieve better parts hardness.

On other hand building the parts in flat orientation making the layers in parallel alignment with the print platform. This is frequently the orientation of the subjected loads in numerous applications, and that reduces the stresses concentration and enhances the layers bonding, leading

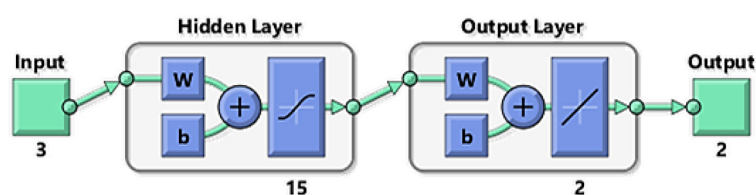
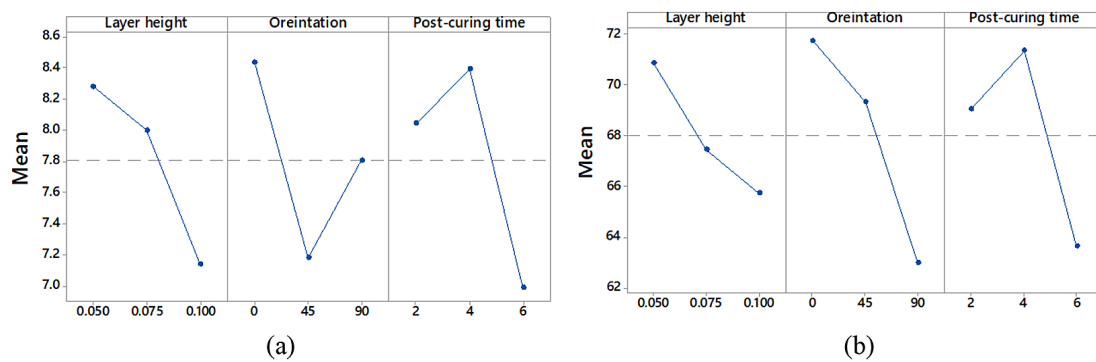


Figure 6. Neural network architecture

**Table 2.** Experiments result of the impact and hardness tests

No.	Layer height (mm)	Build orientation (deg)	Post-curing time (sec)	Impact strengt (KJ/m <sup>2</sup> )	Shore D hardness (HD)
1	0.050	0	4	9.49	77.92
2	0.075	90	2	8.24	63.48
3	0.075	0	2	8.86	72.22
4	0.050	45	2	7.89	73.21
5	0.075	0	6	7.81	66.81
6	0.100	0	4	8.35	72.79
7	0.050	90	4	8.87	69.18
8	0.050	90	6	7.46	61.49
9	0.050	0	2	9.14	75.63
10	0.075	0	4	9.21	74.51
11	0.050	90	2	8.52	66.89
12	0.100	0	2	8.01	70.50
13	0.100	90	6	6.33	56.36
14	0.075	45	6	6.56	64.39
15	0.050	0	6	8.09	70.23
16	0.075	90	6	7.18	58.07
17	0.075	45	4	7.96	72.09
18	0.075	90	4	8.58	65.77
19	0.050	45	6	6.84	67.80
20	0.100	0	6	6.95	65.09
21	0.100	45	6	5.70	62.67
22	0.100	90	4	7.73	64.05
23	0.075	45	2	7.61	69.79
24	0.100	45	2	6.75	68.08
25	0.100	45	4	7.10	70.37
26	0.050	45	4	8.24	75.50
27	0.100	90	2	7.38	61.76



**Figure 7.** Main effects plot for the parts strengths, (a) impact behavior (b) hardness behavior

to improve the impact strength of the parts. The anisotropic nature is reduced in the flat position which enhances the consistency and the uniformity of the mechanical characteristics of the fabricated parts and improves its hardness. The two responses surface plots corresponding to their

effecting parameters illustrated in Figure 8 showing the impact strengths and hardness performance that represented with different pairs of process parameters effect. It is noted that both characteristics increased in flat position, lower layer thickness, and the moderate post curing time.

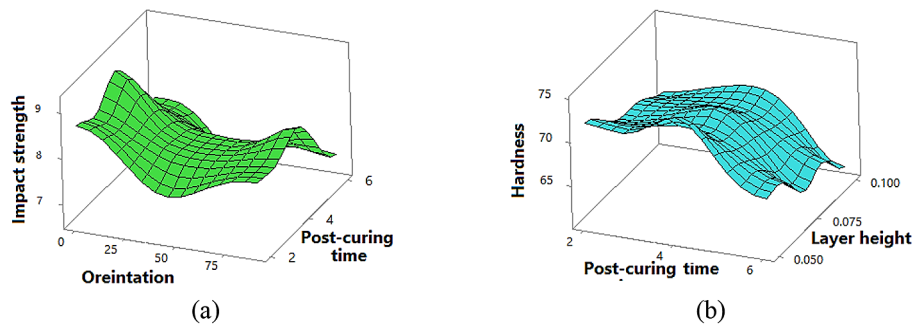


**Figure 8.** Surface plot of the outputs with respect to their inputs, (a) impact strength versus orientation and post-curing time (b) hardness versus layer height and post-curing time

**Table 3.** Analysis of variance result of impact strength

Source	DOF	Sum of squares	Variance	F-value	Contribution %
Layer height	2	6.211	3.156	4.55	27.50
Build orientation	2	7.031	3.52	5.31	30.68
Post-curing time	2	9.50	4.80	8.63	41.83
Error	20	0.21	0.105		
Total	26	22.952			

The contribution weightiness for the input variables on the impact strength and hardness have been examined using ANOVA analysis for determining the significant degree of the investigated variables on the process outcome. From the Tables 3, and 4 of ANOVA analysis, post curing time was the most effective variable on impact strength with 41.83% while build orientation was the most influential parameter on the part hardness. Layer thickness has the lower effect on the two responses.

**Neural network results**

To assess the extent to which the model outputs match the results of the experimental tests, correlation coefficient was utilized for this purpose. This statistical measure can be formulated as [23]:

$$R = \frac{\sum(x_i - \bar{x})(y_i - \bar{y})}{\sqrt{\sum(x_i - \bar{x})^2 \sum(y_i - \bar{y})^2}} \quad (1)$$

Table 5 reveals the agreements between experimental values for impact strength and hardness with ANN model values for the two responses to assess the significance of network topology, transfer functions at the hidden and output layer. The best value of overall R (0.998) has been obtained by using the Levenberg-Marquardt algorithm as shown in Figure 9. While training, the data reaches its maximum optimal solution at epoch 8 and when validation samples MSE start increasing, the epochs automatically stop as shown in Figure 10. The responses’ outputs of the ANN developed models have coefficients of correlation using Equation 1 equal to 0.989 for impact strength and 0.982 for hardness (Figure 11).

For validating the neural network (ANN) model, the mean absolute error between the measurement results and the predicted outcomes was determined in statistical terms. The confidence interval has been calculated for the responses based on the following formula [24]:

**Table 4.** Analysis of variance result of shore D hardness

Source	DOF	Sum of squares	Variance	F-value	Contribution %
Layer height	2	112.8	61.40	2.28	15.94
Build orientation	2	364.5	183.25	10.89	47.57
Post-curing time	2	271.1	140.55	6.89	36.49
Error	20	22.1	11.05		
Total	26	770.5			

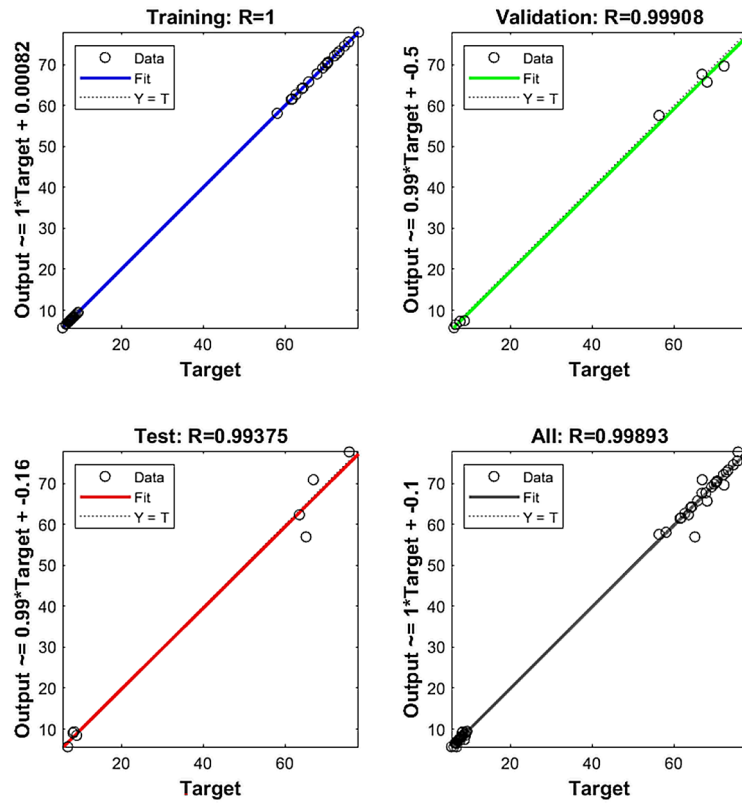


Figure 9. Regression plot for ANN



Figure 10. Mean square error plot for ANN

$$CI = \bar{y} \pm z \frac{s}{\sqrt{n}} \quad (2)$$

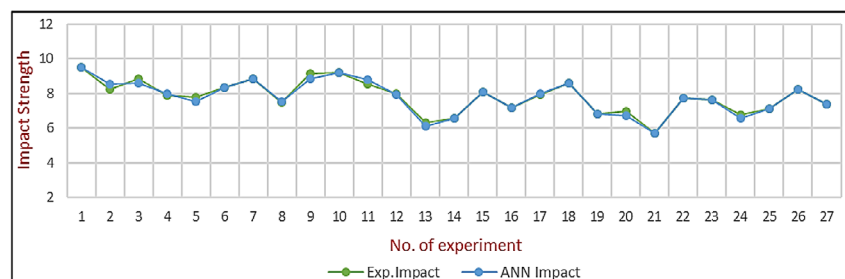
where:  $\bar{y}$  is the mean value,  $z$  is confidence level,  $s$  is standard deviation, and  $n$  is the sample size.

The izod-impact strength has a mean error (1.13%) with a confidence interval (95%) of

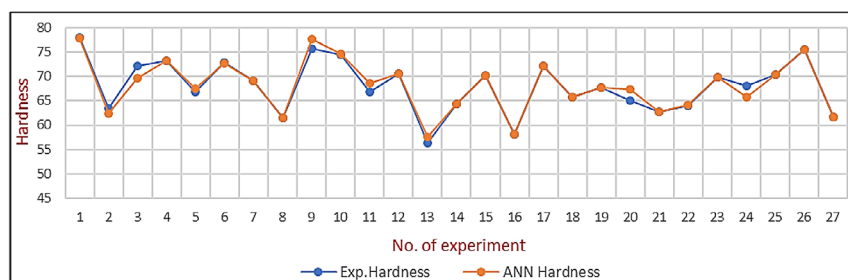
(0.55% to 1.71%), on the other hand the Shore-D hardness has a mean error (0.82%) with a confidence interval (95%) of (0.32% to 1.31%). Both error rates for predictions are of statistical significance  $p < 0.05$ , demonstrating the neural network model's consistency and predictability. The neural network model was used also for

**Table 5.** Experimental data and predicted values

No. of Run	Experimental impact strength (kg/m <sup>2</sup> )	ANN Impact strength (kg/m <sup>2</sup> )	Error (%)	Experimental hardness (HD)	ANN hardness (HD)	Error (%)
1	9.49	9.48	0.06	77.92	77.91	0.02
2	8.24	8.55	3.81	63.48	62.35	1.77
3	8.86	8.61	2.83	72.22	69.61	3.60
4	7.89	7.97	0.99	73.21	73.29	0.11
5	7.81	7.51	3.79	66.81	67.61	1.20
6	8.35	8.36	0.04	72.79	72.77	0.03
7	8.87	8.87	0.03	69.18	69.18	0.01
8	7.46	7.51	0.56	61.49	61.45	0.06
9	9.14	8.83	3.42	75.63	77.69	2.72
10	9.21	9.21	0.06	74.51	74.57	0.08
11	8.52	8.78	3.07	66.89	68.53	2.45
12	8.01	7.95	0.63	70.50	70.63	0.18
13	6.33	6.12	3.27	56.36	57.57	2.15
14	6.56	6.56	0.06	64.39	64.33	0.09
15	8.09	8.09	0.00	70.23	70.19	0.05
16	7.18	7.17	0.15	58.07	58.08	0.02
17	7.96	7.97	0.17	72.09	72.16	0.10
18	8.58	8.58	0.09	65.77	65.79	0.03
19	6.84	6.84	0.00	67.80	67.70	0.15
20	6.95	6.73	3.18	65.09	67.31	3.40
21	5.70	5.71	0.18	62.67	62.69	0.02
22	7.73	7.72	0.18	64.05	64.09	0.05
23	7.61	7.62	0.16	69.79	69.81	0.03
24	6.75	6.55	3.03	68.08	65.73	3.45
25	7.10	7.12	0.20	70.37	70.43	0.09
26	8.24	8.23	0.07	75.50	75.50	0.00
27	7.38	7.35	0.36	61.76	61.64	0.19



(a)



(b)

**Figure 11.** Comparison between experimental and ANN model data: (a) impact strength, (b) hardness

**Table 6.** Optimal printing variables and their corresponding optimal values for impact strength and hardness

Response	Layer height (mm)	Orientation (degree)	Post-curing time (min)	Optimal values
Impact strength	0.053	0°	3.8	9.48 kJ/m <sup>2</sup>
Harness	0.048	0°	4.1	77.91 HD

optimizing the LCD parameters. An algorithm using MATLAB software was created for finding the optimum process parameters that give highest impact strength and hardness. The functions generate 3 vectors, each one of them save (100 elements). The first-vector is for layer height with an interval of 0.05–0.1, the second vector represents the build orientation with interval of 0–90°, and the third vector is dedicated to the post-curing time with interval of 2–6. Furthermore, the algorithm builds pair of three-dimensional array sizes (100 elements in each dimension). The calculated result of the four inputs vectors combination was saved in the first array at the same time for the impact strength. In addition to store the calculations of the hardness strength in the second array. The highest number in each array is the optimum value for the impact strength and hardness, and the corresponding parameters represent the optimum condition of printing. Table 6 illustrates the optimum parameters combinations and their correspondent impact strength and hardness. Clearly, it is observed that the optimal input parameters are almost similar for (*Is*) and (*HD*).

It is important to note that, although the complete replicates weren't conducted on every experimental combination, a portion of the samples were replicated to assess the reliability of measurements, these selective replications validate the reported variations and reinforce the accuracy of the ANNs model's prediction. However, it is certainly preferable to do full repetitions.

## CONCLUSIONS

In the present study, a neural-network model was developed for predicting and optimizing the impact strength, and hardness of the LCD printed parts. Fabricating the samples was performed according to full factorial design of experiments for investigating the influence of layer height, build orientation, and post-curing time as the LCD input variables on part impact strength and parts hardness. The results showed that maximum impact strength and hardness strength are obtained in lower layer height (0.05 mm), flat build position

(0°), and moderate post-curing time (4 min) for impact strength and hardness. Based on the ANOVA analysis, it is found that post-curing time is the most influential variable on impact strength with 41.8%, on the other hand the build orientation has the highest effect on the parts hardness with 47.5%. The developed optimization algorithm was built by incorporating the ANN model through creating three-dimensional array sizes (100 elements in each dimension) to obtain the highest values for the responses which were 9.48 kJ/m<sup>2</sup> and 77.91 HD for the impact strength and hardness, respectively. The adopted model for the investigated mechanical properties showed good agreements with the experiments' outcome with mean error percentage 1.13%, and 0.82% for the impact and hardness, respectively. And it demonstrates outstanding precision for predictions with correlation coefficients 0.989 and 0.982 for the process outputs, respectively. The results reported indicate that the model is capable not just of predicting accurately, but also of effectively optimizing printing variables for better components qualities. Such model of prediction lowers the necessity for significant trial and error testing. It can indicate that neural network models are efficient machine learning tools for predicting the mechanical properties of LCD-printed parts. Future research could extend the utilized method to different performance geometries, and materials in addition to investigating hybrid-AI strategies for multi objective optimizations.

## REFERENCES

1. Paral S. K., Lin D.-Z., Cheng Y.-L., Lin S.-C., and Jeng J.-Y. A review of critical issues in high-speed vat photopolymerization, *Polymers (Basel)*, 2023; 15(12): 2716, <https://doi.org/10.3390/polym15122716>
2. Abdulridha H. H. and Abbas T. F. Analysis and investigation the effect of the printing parameters on the mechanical and physical properties of PLA parts fabricated via FDM printing, *Adv. Sci. Technol. Res. J.*, 2023; 17: 6. <https://doi.org/10.12913/22998624/173562>

3. Quan H., Zhang T., Xu H., Luo S., Nie J., and Zhu X. Photo-curing 3D printing technique and its challenges, *Bioact. Mater.*, 2020; 5(1): 110–115. <https://doi.org/10.1016/j.bioactmat.2019.12.003>
4. Zhu Y. et al. Recent advancements and applications in 3D printing of functional optics, *Addit. Manuf.*, 2022; 52: 102682. <https://doi.org/10.1016/j.addma.2022.102682>
5. Caplins B. W. et al. Characterizing light engine uniformity and its influence on liquid crystal display based vat photopolymerization printing, *Addit. Manuf.*, 2023; 62: 103381. <https://doi.org/10.1016/j.addma.2022.103381>
6. Hu G. et al. Photopolymerisable liquid crystals for additive manufacturing, *Addit. Manuf.*, 2022; 55: 102861. <https://doi.org/10.1016/j.addma.2022.102861>
7. Yang T. and Gu F. Overview of modulation techniques for spatially structured-light 3D imaging, *Opt. Laser Technol.*, 2024; 169: 110037. <https://doi.org/10.1016/j.optlastec.2023.110037>
8. Tosto C. et al. Epoxy based blends for additive manufacturing by liquid crystal display (LCD) printing: The effect of blending and dual curing on daylight curable resins, *Polymers (Basel)*, 2020; 12(7), 1594. <https://doi.org/10.3390/polym12071594>
9. Salih R. M., Kadauw A., Zeidler H., and Aliyev R. Investigation of LCD 3D Printing of Carbon Fiber Composites by Utilising Central Composite Design, *J. Manuf. Mater. Process.*, 2023; 7(2): 58. <https://doi.org/10.3390/jmmp7020058>
10. Dey A. and Yodo N. A systematic survey of FDM process parameter optimization and their influence on part characteristics, *J. Manuf. Mater. Process.*, 2019; 3(3). <https://doi.org/10.3390/jmmp3030064>
11. Abdulrazaq M. M., AL-Khafaji M. M. H., and Kadauw A. The influence of slicing parameters on mechanical strength of FDM printed parts: A review, in *AIP Conference Proceedings*, AIP Publishing, 2025. <https://doi.org/10.1063/5.0254289>
12. Riyaz Ahmed A. and Mugendiran V. Effect of process parameters on mechanical properties of PLA resin through LCD 3D printing, *Proc. Inst. Mech. Eng. Part E J. Process Mech. Eng.*, 2024; 09544089231225147. <https://doi.org/10.1177/09544089231225147>
13. Al-Dulajjan Y. A. et al. Effect of printing orientation and postcuring time on the flexural strength of 3D-printed resins, *J. Prosthodont.*, 2023; 32(S1): 45–52. <https://doi.org/10.1111/jopr.13572>
14. Seprianto D., Sugiantoro R., and Erwin M. The effect of rectangular parallel key manufacturing process parameters made with stereolithography DLP 3D printer technology against impact strength, in *Journal of Physics: Conference Series*, IOP Publishing, 2020, 12028. <https://doi.org/10.1088/1742-6596/1500/1/012028>
15. Yang Y., Zhou Y., Lin X., Yang Q., and Yang G. Printability of external and internal structures based on digital light processing 3D printing technique, *Pharmaceutics*, 2020; 12(3), 207. <https://doi.org/10.3390/pharmaceutics12030207>
16. Schittecatte L., Geertsen V., Bonamy D., Nguyen T., and Guenoun P. From resin formulation and process parameters to the final mechanical properties of 3D printed acrylate materials, *MRS Commun.*, 2023; 13(3), 357–377. <https://doi.org/10.1016/j.heliyon.2018.e00938>
17. Al-Wswasi M., Al-Khaleeli W. A. and Aufy S. A. Implement the artificial neural network concept for predicting the mechanical properties of printed polylactic acid parts, *Adv. Sci. Technol. Res. J.*, 2025; 19(5): 73–83. <https://doi.org/10.12913/22998624/201463>
18. Al-Bdairy A. M. J., Ghazi S. K. and Abed A. H. Prediction of the mechanical properties for 3D printed rapid prototypes based on artificial neural network, *Adv. Sci. Technol. Res. J.*, 2025; 19(3), 96–107. <https://doi.org/10.12913/22998624/197405>
19. Abiodun O. I., Jantan A., Omolara A. E., Dada K. V., Mohamed N. A. and Arshad H. State-of-the-art in artificial neural network applications: A survey, *Heliyon*, 2018; 4(11), e00938. <https://doi.org/10.1016/j.heliyon.2018.e00938>
20. Mahmood M. A., Visan A. I., Ristoscu C. and Mihai-lescu I. N. Artificial neural network algorithms for 3D printing, *Materials (Basel)*, 2020; 14(1), 163. <https://doi.org/10.3390/ma14010163>
21. Al-Shathr A., Shakor Z. M., Majdi H. S., Abdul Razak A. A. and Albayati T. M. Comparison between artificial neural network and rigorous mathematical model in simulation of industrial heavy naphtha reforming process, *Catalysts*, 2021; 11(9), 1034. <https://doi.org/10.3390/catal11091034>
22. Shirmohammadi M., Goushchi S. J., and Keshtiban P. M. Optimization of 3D printing process parameters to minimize surface roughness with hybrid artificial neural network model and particle swarm algorithm, *Prog. Addit. Manuf.*, 2021; 6: 199–215. <https://doi.org/10.1007/s40964-021-00166-6>
23. Abdulrazaq M. M., Al-Khafaji M. M. H., Kadauw A., Krinke S., and Zeidler H. Out-of-position bead geometry prediction in wire arc additive manufacturing (WAAM) using fuzzy logic-based system, *Manag. Syst. Prod. Eng.*, 2025. <https://doi.org/10.2478/mspe-2025-0005>
24. Abdullah M. A., Abed A. H., and Mansor K. K. Comparison between low-carbon steel and galvanized steel by deep drawing under the influence of different parameters, *Manag. Syst. Prod. Eng.*, 2025. <https://doi.org/10.2478/MSPE-2025-0016>